

Figure 3: 499-MHz coaxial type RF deflector made of four $\lambda/4$ transmission lines in a two-cell configuration [4].

(ERL) beam line and the existing Rare Isotope Beam (RIB) program [5]. Owing to the compact shape of the RF Dipole topology, described in the later sections, this cavity was machined from reactor grade bulk Niobium for economical means of fabrication. Prototype results showed promising results towards final use of such a device in the future [6].

RF deflectors at the CLIC Test Facility 3 (CTF3) at CERN were studied to demonstrate the feasibility of the RF power generation through bunch recombination [7]. The technique uses a novel scheme with a delay loop to combine a long bunch train by interleaving the "even" and "odd" bunches into a short train to reduce the bunch spacing by a factor of 2 (see Fig. 4). This recombination is achieved by a fast deflector operating at 1.499 GHz. A second stage was proposed to further compress the bunches with a second combiner ring to achieve a full compression up to a factor of 10. The proposal was tested using two identical TM_{110} standing wave cavities powered with a single RF amplifier through a 90° RF hybrid.

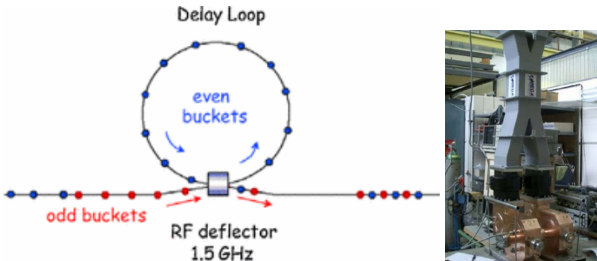


Figure 4: TM_{110} type deflecting structures for recombination of the extracted bunches for reduction of bunch spacing [7].

BUNCH MANIPULATIONS FOR LIGHT SOURCES

Short X-ray pulses with high average flux from conventional light sources can be enabled using RF deflectors in the crabbing phase without reducing the bunch length. One such proposal uses two RF deflectors in TM_{110} mode to create vertical displacements of the electrons correlated to their longitudinal positions [8]. When such a crabbed bunch passes through an undulator it produces an angle dependent divergence for the emitted x-rays (see Fig. 5). These x-rays can be collimated through a slit to achieve pico-second pulses typically not feasible in conventional light sources. The second cavity placed at π betatron phase advance confines the x-z correlation to a small section of the storage ring.

An alternate technique to generate short X-ray pulses, introduced later, uses the same $x - z$ correlation but with two

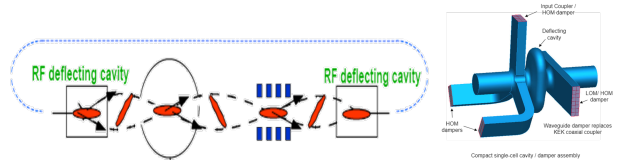


Figure 5: TM_{110} type deflecting structures used to introduce a $x - z$ correlation to introduce divergence in the x-rays and subsequently compress the pulse [8].

different RF frequencies placed next to each other [9, 10]. The frequencies of the two cavities are chosen in such a way that they are spaced by $\frac{1}{2}f_0$:

$$f_1 = nf_0; f_2 = (n + \frac{1}{2})f_0 \quad (2)$$

where f_0 is the main RF frequency, n is an integer harmonic and $f_{1,2}$ are the frequencies of the two RF deflectors. The combined RF wave has the property that half of the RF buckets see the vertical kicks correlated with the longitudinal position in the bunch and the remaining half see no kicks as shown in Fig. 6.

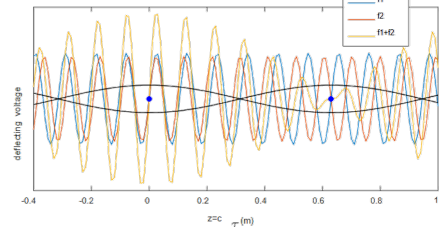


Figure 6: Two-frequency system using TM_{110} type deflecting structures spaced by $1/2$ of a harmonic to create kicks for half the buckets and leave the remaining buckets untouched [9].

Such a scheme with a two frequency system operating at the 6th (3 GHz) and 6.5th (3.25 GHz) harmonic of the main RF system is proposed for the foreseen upgrade of the light source Elettra 2.0 [11]. The use of the two frequency crab cavity system will allow for the production of extreme ultraviolet and X-ray pulses with durations between 0.5 and 5 ps (FWHM) from the insertion devices. The RF cavity design is based on the QMiR deflecting system initially proposed for the Advanced Photon Source (APS) upgrade project [12, 13]. The RF structure consists of a novel concept using multiple transverse electrodes in a waveguide structure (see Fig. 7) to trap the dipole mode used to deflect or crab the electron bunches. The open waveguide structure allows for Higher Order Modes (HOMs) to propagate out of the cavity and does not require dedicated HOM couplers. A single waveguide placed at the cavity center is used to power the cavity with the deflecting mode frequency.

In the Elettra 2.0 upgrade scheme, the kick of the second frequency is split into two symmetric kicks around the center frequency cavity for a better cancellation of the residual transverse kick for the unaffected bunches. Another novel technique uses both higher-harmonic cavities and transverse

cavities to separate the X-ray pulses longitudinally (by generating micro-bunches) and transversely in the undulators, thereby expanding the potential for studies of dynamic processes [14]. The separation in both planes can be tuned with the respective RF parameters.

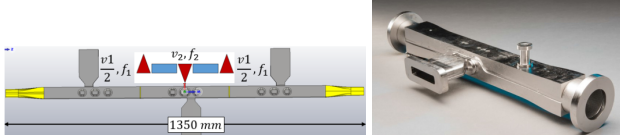


Figure 7: Left: Two-frequency crab cavity system proposed for the Elettra 2.0 upgrade project towards production of ultra-short X-ray pulses [13]. Right: Superconducting QMiR deflecting cavity prototype built for APS upgrade [12].

Emittance exchange between transverse and longitudinal planes using a magnetic chicane and an RF deflector is a valuable technique to reach the small transverse emittances in high-gain Free Electron Lasers (FELs) [15]. A magnetic chicane is used to introduce a dispersive region at the location of the cavity (see Fig. 8). In the RF deflectors, the beam receives a time-dependent transverse kick, leading to a transverse emittance growth while the particles arriving with a transverse offset get a position-dependent energy kick (acceleration or deceleration), thereby reducing the energy spread. It can be shown that after the passage through the chicane and RF deflector, and for the right choice of transverse kick and dispersion (kick = $-1/\eta$), the emittances are exchanged.

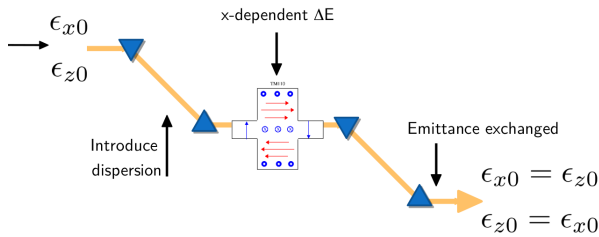


Figure 8: Emittance exchange concept between the transverse and longitudinal planes.

CRAB CROSSING IN COLLIDERS

To confine the collisions in a particle collisions at the center of the detector, the beams are typically transversely separated with a crossing angle (see Fig. 9). The consequence of crossing angle is a reduction of the potential instantaneous luminosity compared to that of a pure head-on collision as depicted in Fig. 9. If the ratio of bunch to the transverse beam size at the interaction point (IP) is much greater than 1, the luminosity reduction can be significant.



Figure 9: Bunches colliding with a crossing angle without crab crossing (left); with the crab crossing (right).

The effective luminosity with a crossing angle can be represented as a Piwinski reduction factor R_Φ given by

$$R_\Phi = \frac{1}{\sqrt{1 + \Phi^2}}. \quad (3)$$

Here, $\Phi = (\sigma_z/\sigma_x^*)\phi$ where ϕ is the half crossing angle and σ_z/σ_x^* is the ratio of the bunch length to the beam size at the collision point.

The beam manipulation at the IP of the colliding beams is used to create optimal collision conditions and maximize the rate of collisions and the luminous region. To recover the overlap, deflecting cavities in a “crabbing” phase were originally proposed by R. Palmer for a geometric compensation for linear colliders [16].

The first crab cavity (superconducting) was proposed and realized for the e^+e^- collider at KEKB in Japan. Two 508.9 MHz crab cavities were successfully constructed and implemented at KEKB [17, 18]. The TM_{110} deflecting mode in a squashed pillbox type cavity was chosen to provide a deflecting voltage of approximately 1.5 MV. A complex mechanism using a coaxial type beam pipe coupler (see Fig. 10) was used to damp both, lower and higher order modes very strongly with a choke at the deflecting frequency. It was also used for electrical centering and as fine tuning mechanism for the deflecting mode.

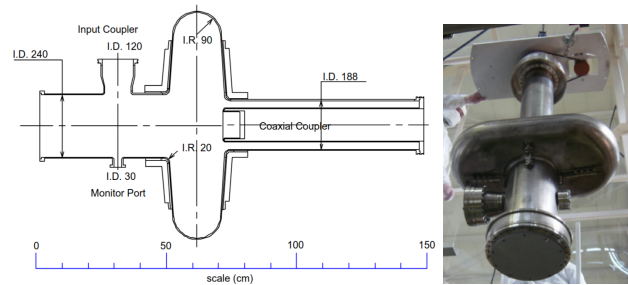


Figure 10: Longitudinal cross section of the KEKB crab cavity with the coaxial damping and tuning mechanism (left) and transverse cross section to depict the elliptical shape to separate the horizontal and vertical dipole mode (right) [18].

The High Luminosity LHC (HL-LHC) will be the first proton collider to use crab cavities to compensate the geometrical luminosity loss from a finite crossing angle to suppress parasitic collisions. The aspect ratios between longitudinal and transverse beam sizes in the HL-LHC span over four orders of magnitude. These large ratios make the Piwinski reduction factor significant and leads to loss of peak luminosity up to 70%.

The high transverse voltage required for the proton beams in the HL-LHC and the very limited space between the two counter-rotating beams led to the development of very compact cavities. Since the crossing planes at the two high luminosity experiments of ATLAS and CMS are different, two cavity geometries (see Fig. 11), the RF dipole and the double-quarter wave geometries are used for the horizontal and vertical crabbing respectively [19].

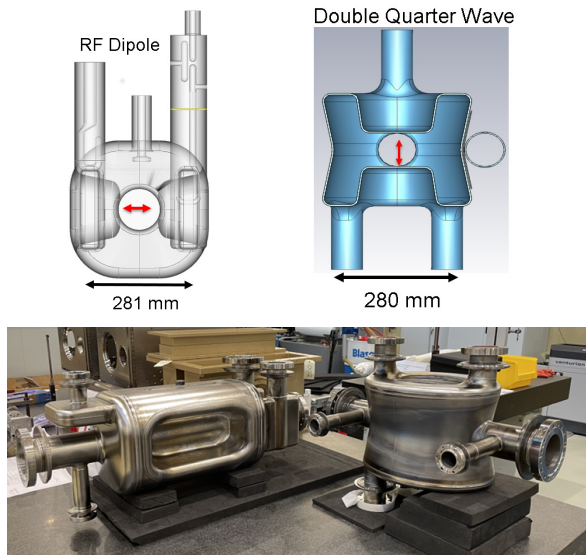


Figure 11: The RF dipole (left) and double quarter wave (right) crab cavity geometries for the HL-LHC.

Very strong HOM damping with several couplers is required to stay within the tight impedance budget of the HL-LHC. Both cavity types were successfully prototyped and tested in the SPS machine with protons for demonstration before the final implementation in the HL-LHC [20]. RF noise related transverse emittance growth from crab cavities in the HL-LHC has been a focus over some years. Several dedicated beam studies in the SPS with crab cavities were carried out to successfully benchmark the effect of RF noise on a proton beam [20, 21]. A dedicated noise feedback system using special stripline BPMs and the crab cavity system is being developed to mitigate the emittance growth to within the specified budget for HL-LHC [21].

The electron-ion collider (EIC) will collide the electron and hadron beams with a horizontal crossing of 25 mrad, similar to the scheme of HL-LHC [22]. The crab cavities are used to tilt both the hadron and electron beams to reach the high beam-beam parameter and achieve the luminosity goals. The proposed crab cavity system is comprised of two frequencies for the hadron beam. The primary at 197 MHz (see Fig. 12) and a second harmonic at 394 MHz to linearize the crab cavity kick and suppress higher-order synchro-betatron resonances [23]. The electron beam is crabbed only with a single frequency at 394 MHz and the bunch length is much smaller than the RF wavelength. Both frequencies use the RF-dipole like topology developed (see Fig. 12) for the HL-LHC project with special dog-bone waveguides to couple both horizontally and vertically for powering the crabbing mode and damping the HOMs strongly. RF noise induced emittance growth remains one of the key issues for the implementation of crab crossing at EIC.

The 14 mrad geometric crossing angle in the superconducting ILC's interaction region requires crab crossing as a baseline to maximize the luminosity. The early baseline used four 9-cell squashed elliptical cavities in the TM_{110} mode, similar to KEKB, to achieve the kick necessary for the 1 TeV

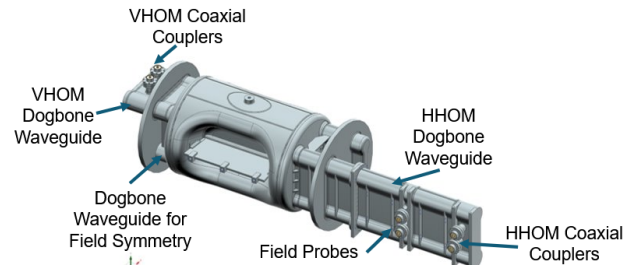


Figure 12: The RF dipole cavity at 197 MHz developed designed for the EIC [23].

center-of-mass collisions [24]. New efforts in exploring designs based on the developments for light sources and HL-LHC lead to several alternatives. Among the five concepts proposed, two designs were retained for further R&D. The first design has an operating frequency of 1.3 GHz and is of the RF dipole type structure (see Fig. 13 top) with coaxial type HOM ILC couplers [25]. The second design is of the QMiR type quasi-waveguide structure with electrodes (see Fig. 13 bottom) to operate at 2.6 GHz.

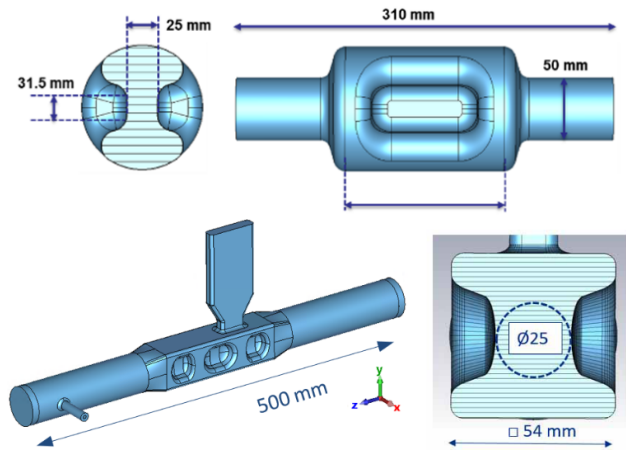


Figure 13: The two crab cavity geometries considered for the future ILC, RFD dipole cavity at 1.3 GHz (top) and QMiR cavity at 2.6 GHz (bottom).

For the normal conducting linear collider study (CLIC), a normal conducting traveling wave structure at X-band (12 GHz) in the TM_{110} were studied and prototyped to investigate their high power performance and breakdown behavior [26].

BEAM DIAGNOSTICS

Transverse deflecting cavities have been extensively used in longitudinal and transverse phase space diagnostics, in particular for single-pass high temporal resolution applications. In the classical approach, the longitudinal phase space is mapped to the transverse plane, where the distribution can be reconstructed using a screen or a similar diagnostic device downstream [27–29]. Traditionally, S-band traveling wave structures (LOLA) at frequencies of 2.856 GHz were used to measure bunch lengths of 10's femto-seconds, for example at the SLAC LCLS accelerator (see Fig. 14).

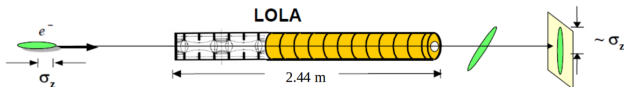


Figure 14: Classical method for bunch length measurement using RF deflector mapped to the transverse plane on a screen.

For even shorter bunch length measurements in FELs requiring sub-femto second resolutions, higher frequency deflecting cavities at 11.45 GHz are necessary, for example the XTCAV also at the LCLS (see Fig. 14). A resolution in of 1 fs r.m.s. was already demonstrated [30]. An additional dipole downstream the deflecting cavity is used to carry out an energy loss scan for measuring x-ray pulse as a function of time (see Fig. 15). The dipole acts as a spectrometer translating energy into a transverse coordinate for a time-energy phase space diagnostic.

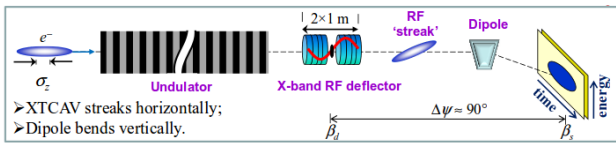


Figure 15: Higher frequency deflecting cavity for sub-femto second temporal diagnostics in conjunction with a dipole spectrometer [27, 28].

Using the RF deflectors in conjunction with a quadrupole downstream to adjust the optics as a function of deflecting voltage allows for a measurement of transverse emittance along the bunch or the momentum spread at dispersive regions [31].

An extension of the X-band diagnostics was proposed to allow for a variable control of the azimuthal angle of the deflection using a polarizable X-band transverse deflecting structure known as PolariX [32]. A novel RF structure was proposed to horizontally or vertically polarize the TE_{11} input signal which is launched into the RF deflector to excite two degenerate deflecting modes by varying the RF phase [33]. Such a system allows for the possibility of 6D characterization and 3D charge distributions in conjunction with tomographic reconstructions (see Fig. 16). A polarizable system is proposed at various facilities at DESY, PSI and other laboratories [32].

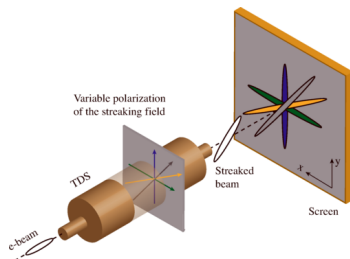


Figure 16: Bunch diagnostics with RF deflectors with variable polarization [32].

Transverse diagnostics using cavity BPMs for very high resolution measurements have been proposed and implemented [34, 35]. The TM_{110} mode is used to measure the

beam position by finding the electrical null where the beam induced voltage is minimum. Specially polarized waveguides to only pick up only dipole mode in both planes are preferred to suppress the parasitic modes including the main TM_{010} mode in the cavity (see Fig. 17). Such a system allows position measurements in the 10–100-nm level required in FELs which is typically not easy to achieve with classical BPMs, especially in a single-pass. Signals from cavity dipole HOMs have also been used as wakefield monitors for beam offset measurements [36].

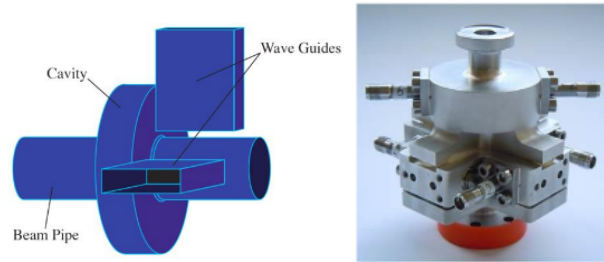


Figure 17: Waveguide-loaded common-mode free cavity BPM design and prototype [35].

CONCLUSIONS

A wide variety of applications for RF deflectors ranging from particle species separation, X-ray pulse compression, crab crossing for luminosity production and beam diagnostics in the present and future accelerators were outlined. For each of the applications some aspects of the RF structure design and challenges were described. Deflecting and crabbing structures have evolved significantly from a very few, one-off application to essential building blocks of most future accelerators. The emergence of new concepts to provide the deflecting or crabbing fields has fundamentally changed the outlook towards the use of such structures. The need for ever higher performances and precision have significantly pushed the boundaries of the technological state-of-the-art to realize them.

REFERENCES

- [1] B. W. Montague, “RF Particle Separators”, CERN, Geneva, Switzerland, Rep. CERN-AR-Int-Psep-63-7, 1963.
- [2] A. Citron *et al.*, “The Karlsruhe-CERN Superconducting RF Separator”, *Nucl. Instrum. Methods*, vol. 164, no. 1, pp. 31–55, Aug. 1979. doi:10.1016/0029-554X(79)90432-4
- [3] OKA experimental program, IHEP, Protvino.
- [4] C. Hovater, “The CEBAF RF Separator System”, in *Proc. CAS-CERN Accelerator School: Radio-frequency Engineering*, CERN, Geneva, Switzerland, 1996, Rep. CERN-96-07, pp. 77–84. doi:10.5170/CERN-1996-007.77
- [5] D. Storey, S. U. De Silva, J. R. Delayen, and R. Laxdal, “Feasibility of an RF Dipole Cavity for the ARIEL e-LINAC SRF Separator”, in *Proc. PAC’13*, Pasadena, CA, USA, Sep.–Oct. 2013, paper MOPAC06, pp. 114–116.
- [6] B. Laxdal, private communication.

- [7] D. Alesini and F. Marcellini, “RF Deflector Design of the CLIC Test Facility CTF3 Delay Loop and Beam Loading Effect Analysis”, *Phys. Rev. ST Accel. Beams*, vol. 12, no. 3, p. 031301, Mar. 2009.
[doi:10.1103/PhysRevSTAB.12.031301](https://doi.org/10.1103/PhysRevSTAB.12.031301)
- [8] A. Zholents *et al.*, “Generation of Subpicosecond X-ray Pulses Using RF Orbit Deflection”, *Nucl. Instrum. Methods Phys. Res., Sect. A*, vol. 425, no. 1–2, pp. 385–389, 1999.
[doi:10.1016/S0168-9002\(98\)01377-1](https://doi.org/10.1016/S0168-9002(98)01377-1)
- [9] A. Zholents, “A New Possibility for Production of Subpicosecond X-ray Pulses Using a Time Dependent Radio Frequency Orbit Deflection”, *Nucl. Instrum. Methods Phys. Res., Sect. A*, vol. 798, p. 111, Oct. 2015.
[doi:10.1016/j.nima.2015.07.025](https://doi.org/10.1016/j.nima.2015.07.025)
- [10] X. Huang *et al.*, “Beam Dynamics Issues for the Two-Frequency Crab-Cavity Short-Pulse Scheme”, *Phys. Rev. Accel. Beams*, vol. 22, no. 9, p. 090703, Sep. 2019.
[doi:10.1103/PhysRevAccelBeams.22.090703](https://doi.org/10.1103/PhysRevAccelBeams.22.090703)
- [11] S. Di Mitri *et al.*, Conceptual Design Study of Crab Cavities for Picosecond X-ray Pulses at ELETTRA 2.0, *to be published*.
- [12] A. Lunin *et al.*, “Design of a Quasi-waveguide Multi-Cell Deflecting Cavity for the Advanced Photon Source”, *Phys. Procedia*, vol. 79, pp. 54–62, 2015.
[doi:10.1016/j.phpro.2015.11.062](https://doi.org/10.1016/j.phpro.2015.11.062)
- [13] N. Shafqat *et al.*, “Crab Cavities at the Elettra 2.0 Storage Ring Light Source”, presented at IPAC’26, Deauville, France, May 2026, paper TUP2002, this conference.
- [14] J. Xu *et al.*, Generation of Tunable Dual X-ray Pulses in Synchrotron Light Sources, *J. Synchro. Rad.*, vol. 32, part 6, p. 1380, Nov. 2025.
- [15] M. Cornacchia and P. Emma, “Transverse to Longitudinal Emittance Exchange”, *Phys. Rev. ST Accel. Beams*, vol. 5, no. 8, p. 084001, Aug. 2002.
[doi:10.1103/PhysRevSTAB.5.084001](https://doi.org/10.1103/PhysRevSTAB.5.084001)
- [16] R. B. Palmer, “Energy Scaling Crab Crossing and the Pair Problem”, SLAC, Menlo Park, CA, USA, Rep. SLAC-PUB-4707, 1988.
- [17] K. Oide and K. Yokoya, “Beam-Beam Collision Scheme for Storage-Ring Colliders”, *Phys. Rev. A*, vol. 40, no. 1, pp. 315–316, Jul. 1989.
[doi:10.1103/PhysRevA.40.315](https://doi.org/10.1103/PhysRevA.40.315)
- [18] K. Hosoyama *et al.*, “Crab cavity for KEKB”, in *Proc. SRF’95*, Gif-sur-Yvette, France, Oct. 1995, paper SRF95F25, pp. 671–675.
- [19] O. Bruning *et al.*, *LHC Design Report*, CERN, Geneva, Switzerland, Rep. CERN-2004-003-V-1, 2004.
[doi:10.5170/CERN-2004-003-V-1](https://doi.org/10.5170/CERN-2004-003-V-1)
- [20] R. Calaga *et al.*, “First Demonstration of the Use of Crab Cavities on Hadron Beams”, *Phys. Rev. Accel. Beams*, vol. 24, no. 6, p. 062001, Jun. 2021.
[doi:10.1103/PhysRevAccelBeams.24.062001](https://doi.org/10.1103/PhysRevAccelBeams.24.062001)
- [21] P. Baudreggien and T. Mastoridis, “RF Stability of the High-Luminosity Large Hadron Collider Crab Cavities”, *Phys. Rev. Accel. Beams*, vol. 27, no. 5, p. 051001, May 2024.
[doi:10.1103/PhysRevAccelBeams.27.051001](https://doi.org/10.1103/PhysRevAccelBeams.27.051001)
- [22] *Electron Ion Collider Conceptual Design Report*, F. Willeke and J. Ye, Eds., Brookhaven National Laboratory, Upton, NY, USA, Feb. 2021. [doi:10.2172/1765663](https://doi.org/10.2172/1765663)
- [23] D. Xu *et al.*, “Study of Harmonic Crab Cavity in EIC Beam-beam Simulation”, in *Proc. IPAC’21*, Campinas, Brazil, May 2021, paper WEPAB009, pp. 2544–2547.
[doi:10.18429/JACoW-IPAC2021-WEPAB009](https://doi.org/10.18429/JACoW-IPAC2021-WEPAB009)
- [24] C. Adolphsen *et al.*, “The International Linear Collider TDR-Volume 3.I: Accelerator R&D in the Technical Design Phase”, *arXiv*, 2013. [doi:10.48550/arxiv.1306.6353](https://doi.org/10.48550/arxiv.1306.6353)
- [25] P. A. McIntosh *et al.*, “Crab Cavities for ILC”, in *Proc. SRF’23*, Grand Rapids, MI, USA, Jun. 2023, pp. 990–998.
[doi:10.18429/JACoW-SRF2023-FRIBA04](https://doi.org/10.18429/JACoW-SRF2023-FRIBA04)
- [26] B. Woolley *et al.*, “High-Gradient Behavior of a Dipole-Mode RF Structure”, *Phys. Rev. Accel. Beams*, vol. 23, no. 12, p. 122002, Dec. 2020.
[doi:10.1103/PhysRevAccelBeams.23.122002](https://doi.org/10.1103/PhysRevAccelBeams.23.122002)
- [27] H. Loos, “Longitudinal Diagnostics for Short Electron Beam”, in *Proc. PAC’09*, Vancouver, BC, Canada, May 2009, paper TU1RBC01, pp. 788–792.
- [28] Y. Ding *et al.*, “Femtosecond X-ray Pulse Temporal Characterization in Free-electron Lasers Using a Transverse Deflector”, *Phys. Rev. ST Accel. Beams*, vol. 14, no. 12, p. 120701, Dec. 2011. [doi:10.1103/PhysRevSTAB.14.120701](https://doi.org/10.1103/PhysRevSTAB.14.120701)
- [29] A. Gillespie, “Bunch Length Diagnostics: Current Status and Future Directions”, 2018 CERN Accelerator School, Tuusula, Finland, *arXiv*, 2018.
[doi:10.48550/arXiv.2005.05715](https://doi.org/10.48550/arXiv.2005.05715)
- [30] C. Behrens *et al.*, “Few-Femtosecond Time-Resolved Measurements of X-ray Free-Electron Lasers”, *Nat. Comm.*, vol. 5, no. 3762, 2014. [doi:10.1038/ncomms4762](https://doi.org/10.1038/ncomms4762)
- [31] M. Röhrs *et al.*, “Slice Emittance Measurements at FLASH”, in *Proc. EPAC’06*, Edinburgh, UK, Jun. 2006, paper MOPCH152, pp. 318–320.
- [32] P. Craievich *et al.*, “Novel X-band Transverse Deflection Structure with Variable Polarization”, *Phys. Rev. Accel. Beams*, vol. 23, no. 11, p. 112001, Nov. 2020.
[doi:10.1103/PhysRevAccelBeams.23.112001](https://doi.org/10.1103/PhysRevAccelBeams.23.112001)
- [33] A. Grudiev, “Design of Compact High Power RF Components at X-Band”, CERN, Geneva, Switzerland, Rep. CLIC-Note-1067, 2016.
- [34] S. Walston *et al.*, “Performance of a High Resolution Cavity Beam Position Monitor System,” *Nucl. Instrum. Meth. Phys. A*, vol. 578, no. 1, pp. 1–22, 2007.
[doi:10.1016/j.nima.2007.04.162](https://doi.org/10.1016/j.nima.2007.04.162)
- [35] J. R. Towler *et al.*, “Development and Test of High Resolution Cavity BPMs for the CLIC Main Beam Linac”, in *Proc. IBIC’15*, Melbourne, Australia, Sep. 2015, pp. 474–478.
[doi:10.18429/JACoW-IBIC2015-TUPB060](https://doi.org/10.18429/JACoW-IBIC2015-TUPB060)
- [36] S. Molloy *et al.*, “High Resolution Cavity Beam Position Monitors for the International Linear Collider”, *Meas. Sci. Technol.*, vol. 18, no. 8, pp. 2314–2324, Aug. 2007.
[doi:10.1088/0957-0233/18/8/007](https://doi.org/10.1088/0957-0233/18/8/007)